

Effects of atomic-force-microscope tip characteristics on measurement of solvation-force oscillations

L. D. Gelb and R. M. Lynden-Bell

University of Cambridge, Department of Chemistry, Lensfield Road, Cambridge CB2 1EW, United Kingdom

(Received 19 July 1993; revised manuscript received 27 September 1993)

We have previously used molecular dynamics to simulate the force oscillations experienced by a model atomic-force-microscope tip brought near a surface under a Lennard-Jones liquid. Here we perform these simulations for additional tip radii. We also apply an Ornstein-Zernicke-type integral equation theory to this system, and obtain force-distance curves for several different state points, tip radii, and surface-liquid potentials. We find this theory to be in good agreement with simulation results for tip-wall separations greater than one molecular diameter. We conclude that the magnitude of the force oscillations experienced by an atomic-force-microscope tip is a linear function of the effective tip radius (at constant temperature) and that measurement of these force curves with a standard solvent could provide a method of estimating the relative radii of different tips.

I. INTRODUCTION

The atomic force microscope provides a technique for imaging surfaces. A sharp tip is moved toward a surface, and the force on the tip is measured. Images may then be obtained by rastering the tip relative to the surface. In such a system, the resolution of these images will be determined by the size of the effective contact area of the tip. Finer tips should yield higher resolutions, but would be more fragile. In these experiments the tip size is not known to any precision, so that the images obtained are much harder to interpret. In this technique, the tip and surface may be immersed in a liquid, in which case solvation forces will contribute to the total measured force. Since the magnitude of the solvation force between two surfaces in a liquid should depend in some way on the "area" of their interaction, measurements of these forces would be very sensitive to tip size. Often a succession of tips is used in the same apparatus, and measurement of these solvation forces could give some indication of the relative sizes of the tips.

O'Shea, Welland, and Rayment¹ have used the atomic force microscope to probe the structure of the liquid-graphite interface for several different liquids. With octamethyltetrasiloxane (OMCTS) they observed force-distance oscillations qualitatively similar to those seen by Horn and Israelachvili.² 1-dodecanol showed a stepped force curve, indicating a layered, liquid-crystal-like structure at the surface, and under water their microscope tip jumped to contact the surface from a separation of about 6 nm. A liquid near a flat surface shows an oscillatory density profile, and so two surfaces brought near to each other should experience a solvation force that oscillates with varying separation, as the oscillations in the density profiles of the solvent around the surfaces move in and out of phase with each other. Several computer simulators have obtained this result for parallel walls enclosing a Lennard-Jones fluid.³⁻⁵ Horn and Israelachvili² have used a surface force apparatus to measure the force oscil-

lations experienced by two crossed mica cylinders in OMCTS, and see a force-distance curve that decays as a simple exponential, with 6-8 visible oscillations. Simulations⁷ show 4-5 oscillations in the density profile of a dense liquid near a wall, so we should not expect to see more than 8-10 oscillations in the force curve, since the layered liquid structure only extends that far away from the wall.

It is less obvious what will happen when a curved or irregular tip approaches a flat surface because the solvent shells of the two surfaces will overlap constructively in some places and destructively in others. In a previous paper⁸ we performed molecular dynamics calculations on a very simple model of the atomic-force-microscope system: a smooth sphere 5σ in diameter brought near a smooth flat surface immersed in a Lennard-Jones fluid. This yielded a force-distance curve qualitatively similar to the experimental result for OMCTS. By looking at the liquid density profiles at varying separations, we have characterized the minima, maxima, and zeros in the force-distance curve as arising from the packing behavior of the liquid immediately under the tip. From these simulations we concluded that, at least for the model studied, the variation of solvation force with separation showed oscillations similar to those seen between parallel plates. The relevant separation is the distance between the surface and the bottom of the tip. The main differences between the results of the parallel surface simulations and ours are that the oscillations decay faster in our microscope model, and that structure is seen in the density distribution in the crevices between the sphere and the flat surface.

In this paper we have extended this work to investigate the effects of tip size, liquid-surface potential, temperature, and liquid density on these force curves. The results we present come from molecular dynamics simulations and from the application of Ornstein-Zernicke-type integral equation theory. This is accomplished via an extension of the method devised by Henderson and

Plischke⁹ to study colloidal suspensions in a simple liquid; we regard the system as composed of two infinitely dilute spherical colloidal particles, one of infinite size (the wall) and one of finite radius (the sphere). We observe force oscillations for a large range of tip curvatures, and conclude that the magnitude of these oscillations varies linearly with the tip radii. We also observe the effects of changing the surface-liquid potential on these force curves, as well as the effects of changing the state point of the liquid.

II. METHODS

A. Molecular dynamics

In our molecular dynamics simulations, the system consisted of a box bounded top and bottom by smooth walls, with periodic boundary conditions in the x and y directions. The box contained a dense fluid and a structureless immobile sphere representing the tip. The fluid particles interact with each other via a cut-and-shifted Lennard-Jones potential:

$$V_{ij}(r_{ij}) = \begin{cases} 4\epsilon \left[\left(\frac{\sigma}{r_{ij}} \right)^{12} - \left(\frac{\sigma}{r_{ij}} \right)^6 \right] - V(r_{\max}) & r_{ij} \leq r_{\max} \\ 0, & r_{ij} > r_{\max} \end{cases} \quad (1)$$

and with the walls via the uncorrugated Steele¹⁰ potential for a (100) face of a face-centered cubic lattice:

$$V_{\text{wall}}(z) = 2\pi\epsilon \left[\frac{2}{5} \left(\frac{\sigma}{z} \right)^{10} - \left(\frac{\sigma}{z} \right)^4 - \frac{\sqrt{2}}{3 \left(\frac{z}{\sigma} + \frac{0.61}{2\sqrt{2}} \right)^3} \right]. \quad (2)$$

The interaction with the sphere is given by

$$V_{\text{sphere}}(r) = 3 \times 4\epsilon \left[\left(\frac{\sigma}{(r - r_{\text{sphere}})} \right)^{12} - \left(\frac{\sigma}{(r - r_{\text{sphere}})} \right)^6 \right] \quad (3)$$

where r_{sphere} is the radius of the large sphere, so that the diameter of the sphere is $2r_{\text{sphere}} + \sigma$. The well depth of this potential is comparable to that of the Steele potential.

Three different systems have been simulated, with sphere diameters of 11σ , 5σ , and 3σ . The simulation box parameters are given in Table I. Only a few separations

TABLE I. Simulation box parameters for the molecular-dynamics calculations.

Diameter of sphere ($2r_{\text{sphere}} + \sigma$)	Box height (σ)	Box width (σ) in x and y directions	Number of particles in box
3.0	12.0	8.0	512
5.0	16.0	10.0	1024
11.0	22.0	17.0	4096

were done with the 11σ -diameter sphere, as it is computationally much more expensive than the others.

In each simulation the density of liquid in the volume at least 2σ away from all surfaces was measured and taken to be approximately the density of the bulk fluid with the same chemical potential as our confined fluid. For all three sets of simulations this value was $\rho^* \approx 0.72$; thus these simulations were performed at comparable state points. This was not an attempt at a precise characterization of the state point of the system (which would require a direct measurement of the chemical potential) but a way to impose consistency on the different simulations.

The simulations were performed at $T^* = 1.0$ using a Berendsen¹¹ thermostat during the equilibration periods. The radial cutoff in the Lennard-Jones potential was taken as 3.5σ . The Verlet¹² algorithm was used to integrate the equations of motion with a time step of 10^{-2} reduced time units. In the simulations, the sphere was moved slowly between one separation and the next (0.25σ over 250 time steps), equilibrated for at least 2000 steps, and then data were gathered for at least 6000 steps. Errors in the accumulated quantities were estimated by averaging separately the first and second halves of each run.

B. Integral equations

To apply integral equation theory to this system, we extend the method of Henderson and Plischke as follows. We consider a ternary fluid mixture, in which the density of two of the species approaches zero, and the size of one of these becomes infinite (giving a wall). Specifically, we would have a liquid with three species present: species 1 (the fluid) of mole fraction $X_1 = 1$; species 2 (the sphere) of finite radius R and mole fraction $X_2 \rightarrow 0$; and species 3 (the wall) of infinite radius, and mole fraction $X_3 \rightarrow 0$. Since all three of these species are spherical, we see that all pair correlation functions $g_{ij}(r_i - r_j)$ are functions of r_{ij} only. Thus the numerical solution of this system will only require discretization of one variable, and will be quite tractable.

We apply the Ornstein-Zernike relations for an isotropic ternary mixture. These are exact relations between the *total correlation function* $h_{ij}(r) = g_{ij}(r) - 1$ [where $g(r)$ is the familiar pair distribution function] and $c_{ij}(r)$, the *direct correlation function*. By applying approximate closure relations to the Ornstein-Zernike relations, we obtain a closed system of integral equations, which are numerically solvable. In general, for an isotropic mixture of N different species, the Ornstein-Zernike relations are¹³

$$h_{ij}(r) = c_{ij}(r) + \rho \sum_{k=1}^N X_k \int h_{ik}(r') c_{kj}(|r - r'|) d^3 r', \quad (4)$$

where i and j are indexes over the different species, X_k is the mole fraction of species k , and ρ is the number density of the mixture. For the system described above, this reduces to

$$h_{11}(r) = c_{11}(r) + \rho \int h_{11}(r') c_{11}(|r - r'|) d^3 r', \quad (5)$$

$$h_{12}(r) = c_{12}(r) + \rho \int h_{11}(r') c_{12}(|r - r'|) d^3 r', \quad (6)$$

$$h_{13}(r) = c_{13}(r) + \rho \int h_{11}(r') c_{13}(|r-r'|) d^3 r', \quad (7)$$

$$h_{23}(r) = c_{23}(r) + \rho \int h_{21}(r') c_{13}(|r-r'|) d^3 r'. \quad (8)$$

(There are, of course, relations for the 22 and 33 functions, and equivalent relations for the 21, 31, and 32 functions, which are identical to the 12, 13 and 23 functions, but they are of no interest at present.) Our goal is to obtain the 23 functions, since from $h_{23}(r)$ we may obtain the force curve between the wall and the sphere from

$$\beta F_{23}(r) = \frac{\partial}{\partial r} \ln[h_{23}(r) + 1]. \quad (9)$$

To use these equations, we must apply (approximate) closures to *each* of the above relations. We have chosen to use the soft-core mean-spherical approximation (SMSA) for the liquid-liquid functions, which is

$$c(r) = 1 - \exp[(V_1(r)][h(r) + 1] - \beta V_2(r)]. \quad (10)$$

This closure divides each potential function $V(r)$ into a short-ranged repulsive part $V_1(r)$ and a long-ranged attractive part $V_2(r)$, and is reputed to be fairly accurate for long-tailed potentials such as the Lennard-Jones (see Hansen and McDonald, *Theory of Simple Liquids*). For the 12, 13, and 23 functions we have applied the so-called hypernetted chain (HNC) approximation, which is

$$c(r) = -\beta V(r) + h(r) - \ln[h(r) + 1]. \quad (11)$$

We use this closure for both the surface-liquid relations because the density profiles $n_{12}(r)$ and $n_{13}(z)$ obtained with the HNC closure better approximated the molecular dynamics results than those obtained with the SMSA closure. Trials with the often-used Percus-Yevick closure applied to the 12 functions resulted in $h_{12}(r)$ functions with negative-valued first minima, which are unphysical, so this closure was rejected. For the wall-sphere functions, either the HNC or Percus-Yevick closure should be appropriate, since the wall-sphere potential is a step function.

To solve these equations, we first obtain the 11 functions (by solving the integral equations for the pure Lennard-Jones fluid), which are then used as input into the equations for the 12 and 23 functions. When we have these, 23 functions can be obtained by a single numerical integration, without the use of any iterative method. We apply Zerah's method¹⁴ to solve for the 11 and 12 functions; this is essentially a Newton-Raphson iteration that uses a conjugate gradient procedure (rather than direct matrix inversion) to solve the linearized system at each step, and is very efficient. To solve for the functions involving the wall we must follow Henderson, Abraham, and Barker¹⁵ and move the coordinate origin to the surface of the large sphere before allowing its radius to become infinite. This results in the following expressions:

$$h_{13}(z) = c_{13}(z) + 2\pi\rho \int_0^\infty t c_{11}(t) dt \int_{z-t}^{z+t} h_{13}(s) ds \quad (12)$$

$$h_{23}(z) = c_{23}(z) + 2\pi\rho \int_0^\infty t c_{21}(t) dt \int_{z-t}^{z+t} h_{13}(s) ds. \quad (13)$$

We solve for the 13 functions using Picard iteration and numerical integration (trapezoid rule). This is much less efficient than Newton-Raphson methods, but is computationally much simpler, and is sufficient for our purposes.

In solving these equations, all functions were discretized over a grid with spacing 0.0469σ . The 11 functions were obtained between $r=0$ and 12σ , the 12 functions were obtained between $r=0$ and 24σ , and the 13 functions were obtained between $r=-12\sigma$ and 12σ , in the manner of Henderson and Plischke. Although we have not used as fine a grid as they, we observed no quantitative differences between using grids of size $\sim 0.10\sigma$ and 0.0469σ , and so are confident that these solutions are accurate.

III. RESULTS

A. Molecular dynamics

In Fig. 1 we present curves of F/R vs separation from the molecular dynamics simulations, where F is the force on the tip, and $R = r_{\text{sphere}} + \sigma/2$ is the effective radius of the sphere. We have divided the data for each curve by the corresponding sphere radius R , in the manner of Horn and Israelachvili. The fact that these curves coincide except at very small separations shows that the force felt by the sphere (at separations greater than $\sim 2\sigma$) is proportional (at least over this range of tip sizes) to its radius, to within the precision of these simulations. In Fig. 2 we plot the amplitudes of the first two force oscillations vs the radius of the tip. Linear regression gives a slope of 84.8 ± 4.2 for the first oscillation, and 19.0 ± 0.7 for the second. This linear behavior is somewhat surprising; one might expect the magnitude of the interaction to vary with the surface area of the sphere, and thus R^2 . Consider the construction in Fig. 3, in which we measure the "flat" part of the bottom of the sphere. It is trivial to show that the width C of this "flat" part is proportional to \sqrt{R} and so its *area* will vary with R :

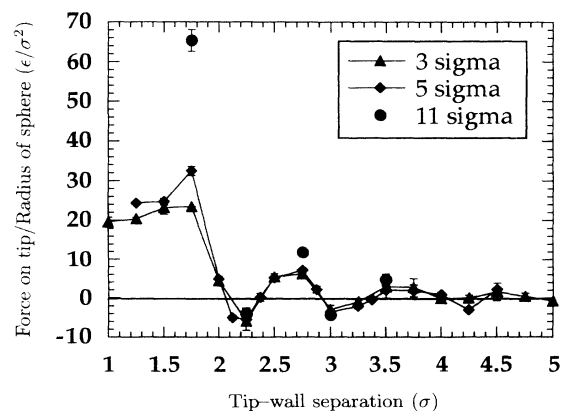


FIG. 1. Force-distance curves from molecular-dynamics simulations of 11σ , 5σ , and 3σ -diameter spheres. The data have been normalized by sphere radius. A positive force indicates repulsion. These are plots of the *average total force* on the sphere; at large separations, they decay to zero as expected.

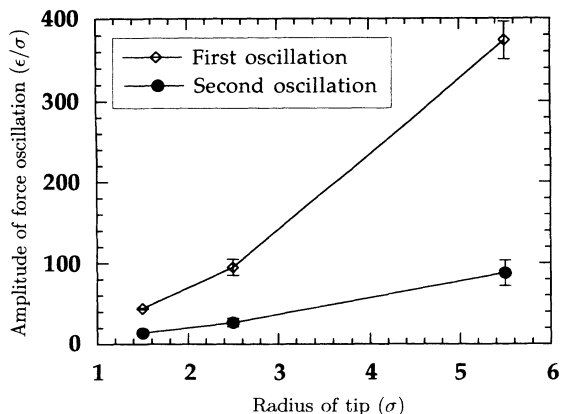


FIG. 2. Molecular dynamics results for the amplitudes of the first two force oscillations vs radius of the sphere. The first oscillation is defined as the first maximum value minus the first minimum value, etc.

$$\begin{aligned}
 R^2 &= C^2 + (R - \delta z)^2, \\
 R^2 &= C^2 + R^2 - 2R\delta z + \delta z^2, \\
 C^2 &= 2R\delta z - \delta z^2.
 \end{aligned}
 \tag{14}$$

That is, to first order in the thickness δz , the contact area will be given by

$$\pi C^2 \cong 2\pi R \delta z. \tag{15}$$

By choosing $\delta z \sim \sigma$ we see that the magnitude of the interaction between a single spherical solvation layer and a single planar solvation layer will vary linearly with the radius of the spherical layer. Because the size of the oscillations in fluid density near the surfaces decay exponentially, the interaction of the layers far from the surfaces will not contribute much to the total force. Thus the contribution of the liquid immediately under the tip should dominate the total force, and so we see this linear behavior. If we look at the limit of large sphere size this becomes even clearer. As $R \rightarrow \infty$ we require that the force per unit area go to a constant value, which is exactly the behavior predicted by this simple construction.

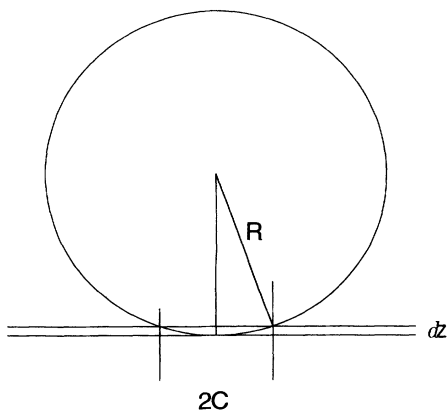


FIG. 3. Geometric construction of the “flat” part of the tip.

Below 2σ separation, however, this linear behavior is not observed; the larger tips experience much larger repulsions at 1.75σ separation. In Fig. 2, we see non-linearity in the data for the first oscillation because the largest tip size experiences a larger force than our construction predicts. This effect is due to the packing of individual solvent molecules under the sphere. At these separations the solvent is excluded from the volume immediately under the sphere, and so our previous argument will not be valid. Instead, the large repulsive force is due to molecules “wedged” into the crevice created by the sphere and surface. Figure 4 shows representative configurations from the three sets of simulations at a tip-wall separation of 1.75σ ; the viewpoint is from the flat surface in the z direction, along the central axis. We see that molecules penetrate quite close to this axis, and only a few are in the volume expected to give the strongest repulsions. Under the largest sphere, *two* rings of single atoms are observed: this may explain the particularly large repulsive force observed, since there are many more particles in this region than for the other spheres. The ringed structures under the 11σ -diameter sphere and close-packed behavior near it are interesting but not surprising; we should expect such behavior from a dense liquid in a deep potential well.

B. Integral equations— comparison with simulations

The integral equation results for the 5σ diameter sphere system are shown with the previous simulation results in Fig. 5. In the integral equation theory, the sharp peak at 1.75σ is absent, and the first minimum is slightly too deep. For larger separations, the agreement is good. We see that the integral equations fail to give the right behavior for separations where the effects of individual “trapped” molecules become important. One of the approximations inherent in our treatment of the system is that the 12 (liquid-sphere) functions are not perturbed by the presence of the wall, and that the 13 (liquid-wall) functions are not perturbed by the presence of the sphere. As we bring the sphere and wall closer together, then, this becomes a more and more severe approximation, and could explain the failure of the theory at very small separations. In general, we can expect this theory to be qualitatively correct for all but the smallest separations, and to be quantitatively correct for separations greater than about 2.5σ .

C. Integral equations— other systems

We use this theory to compare different size spheres. Figure 6 shows the force curves generated by the integral equation theory, for a much larger range of sphere sizes that we were able to simulate by molecular dynamics (MD). Again we see that the range of oscillations is relatively unaffected by the size of the sphere. In Fig. 7 we plot the amplitudes of the first three force oscillations vs the radius of the sphere; it is evident that the linear behavior observed earlier holds for the approximate theory as well. The slope of the line through the points for the first oscillation is 10.45 ± 0.09 , and through the second and third data the slopes are 6.77 ± 0.03 and

4.17 ± 0.03 , respectively. These slopes are much lower than the corresponding data from our MD simulations, due to the failure of this integral equation theory at very small separations.

Figure 8 shows the results of varying the temperature of the system; the bulk fluid density is constant at $\rho^* = 0.73$ for these curves. We see that decreasing the temperature (at least over the range studied) increases the magnitude of the force oscillations, but has no effect on their periodicity, and only a very small effect on their extent away from the wall.

Figure 9 shows the results of varying the liquid density at constant temperature. We see that increasing the den-

sity both increases the magnitude of the force oscillations and also decreases the period; such behavior is to be expected considering our previous packing-oriented explanation of the force oscillations. As we increase the density, we increase the packing fraction and thus decrease the average interparticle distance, which would account for the decreased period of oscillations. This is a situation where the approximate theory and MD calculations may very well show somewhat different trends; this behavior should be very sensitive to the approximation mentioned earlier, that the 12 functions are calculated independently of the presence of the wall, etc., but we have not yet simulated different liquid densities by molecular

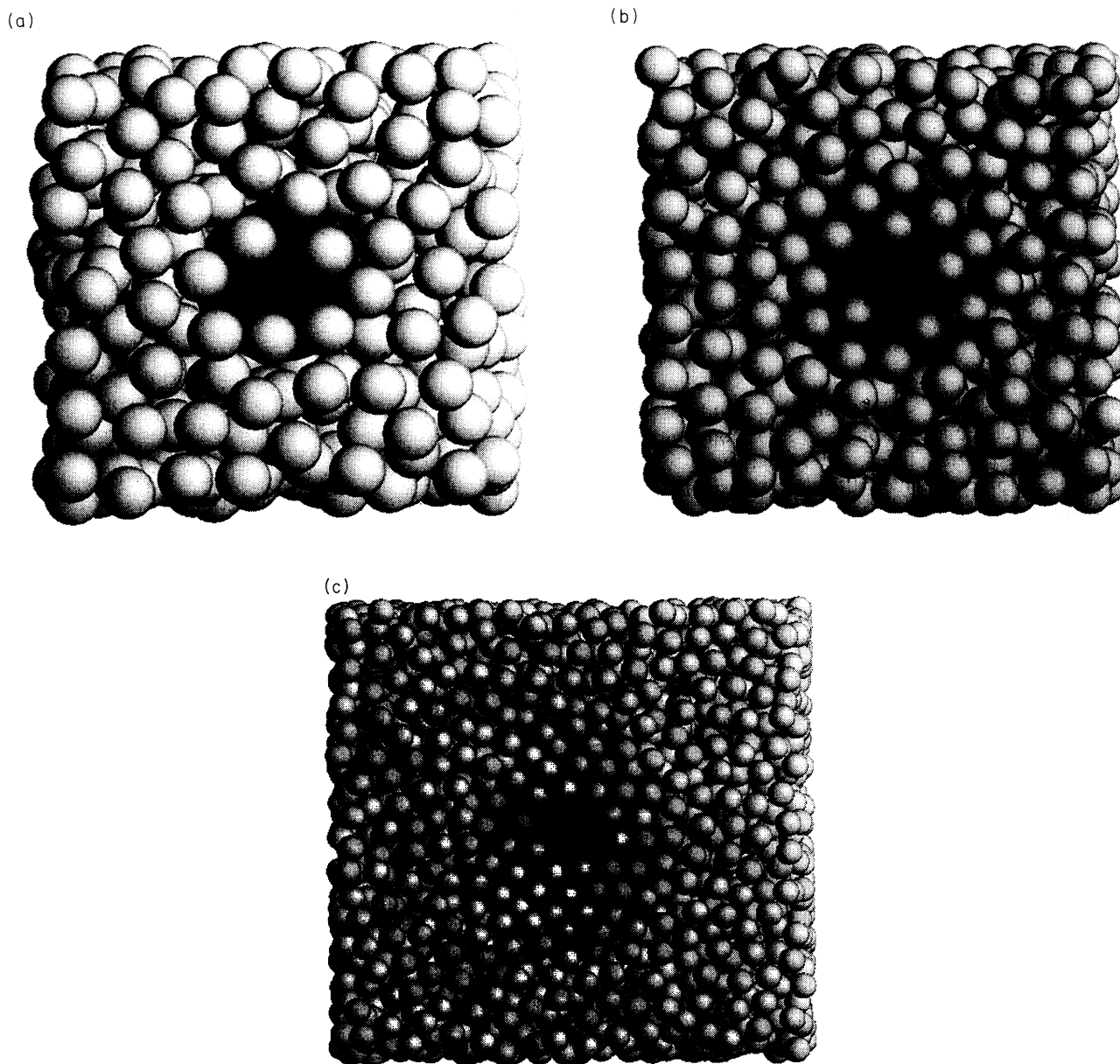


FIG. 4. Representative molecular-dynamics configurations from all three diameter sphere simulations, each at a tip-wall separation of 1.75σ . (a) is from the 3σ diameter sphere run, (b) is from the 5σ sphere run, and (c) is from the 11σ sphere run. In each case, the viewpoint is from the center of the bottom surface, looking up along the z axis. In other words, the topmost layer of visible atoms in each configuration is the first solvation layer alongside the flat surface.

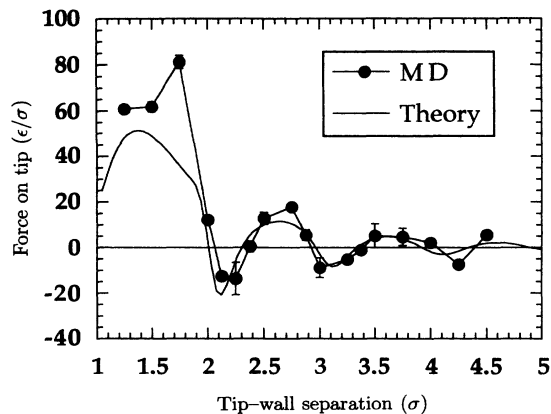


FIG. 5. Force-distance-curves generated by both integral equations and molecular-dynamics simulations for the 5σ -diameter sphere system.

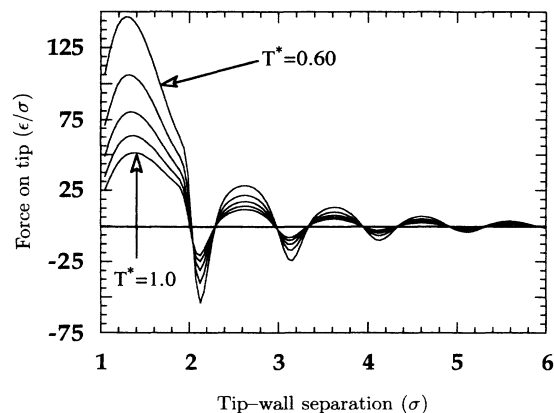


FIG. 8. Effects of varying temperature on force curves at constant liquid density of $\rho^*=0.73$ and sphere diameter of 5σ . The curves shown are at $T^*=0.60, 0.70, 0.80, 0.90,$ and 1.00 . These results were obtained by solving the integral equations.

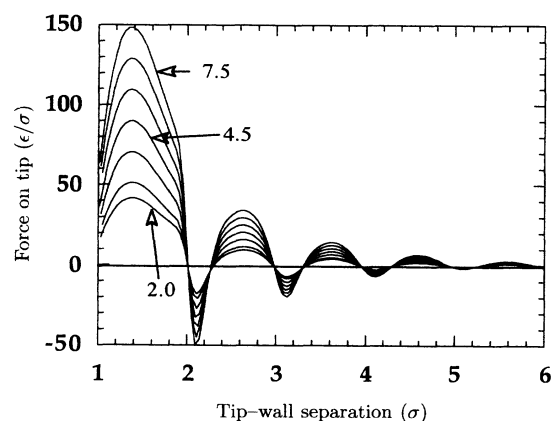


FIG. 6. Force curves for different size spheres, at a bulk liquid reduced density of $\rho^*=0.73$ and a reduced temperature of $T^*=1.0$, obtained from solving the integral equations. The curves shown are for sphere radii of $7.5\sigma, 6.5\sigma, 5.5\sigma, 4.5\sigma, 3.5\sigma, 2.5\sigma,$ and 2.0σ .

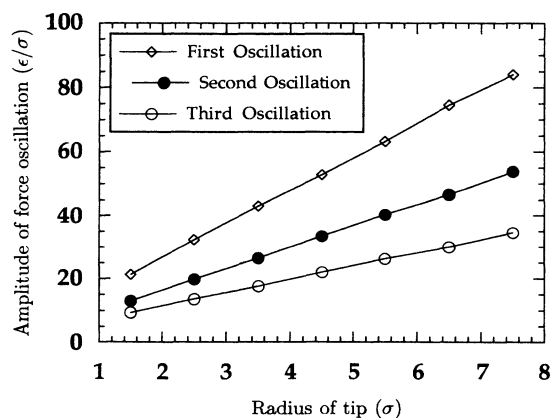


FIG. 7. Amplitudes of the first three force oscillations vs radius of the sphere, for different spheres, at a bulk liquid density of $\rho^*=0.73$ and a reduced temperature of $T^*=1.0$. The first oscillation is defined as the first maximum value minus the first minimum value, etc. These results were obtained by solving the integral equations.

dynamics to see if this is true.

Figure 10 shows the decay with tip-wall separation of the amplitude of the normalized oscillations of the force curves for spheres of diameter 5σ and 11σ as predicted by the integral equation theory. Figure 10 also shows the (normalized) decay rate for the MD simulation of the 3σ -diameter sphere system. These data are not as clean as that obtained from the integral equations, but within errors it also decays exponentially. Horn and Israelachvili have observed this behavior as well, and it arises from the well-known exponential decay of the $h(r)$ functions.

D. Integral equations—hard-wall results

We have also used the integral equation theory to obtain force curves for a system composed of a Lennard-Jones fluid, a hard wall, and a hard sphere. That is, the potentials for the liquid-wall interaction and the liquid-sphere interaction are

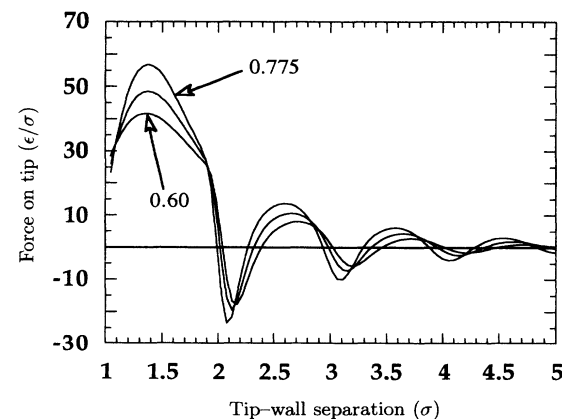


FIG. 9. Effects of varying density on force curves, at a constant temperature of $T^*=1.0$ and sphere diameter of 5σ . The curves shown are at $\rho^*=0.60, 0.70,$ and 0.775 . These results were obtained from solving the integral equations.

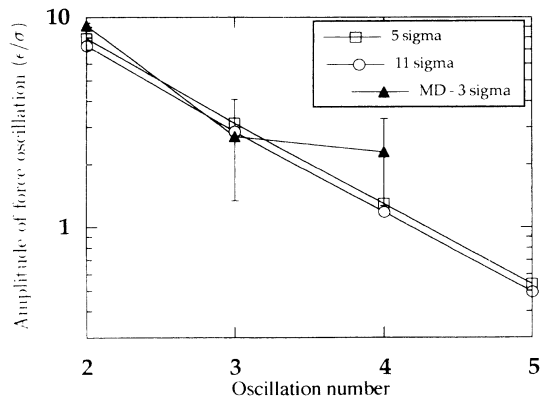


FIG. 10. Variation of the amplitudes of the force oscillations with tip-wall separation. Results for the 3σ -diameter sphere were obtained from molecular-dynamics simulations, while results for the 5σ - and 11σ -diameter spheres were obtained by solving integral equations. The first oscillation is defined as the first maximum value minus the first minimum value, etc. The fifth oscillation was not studied during the molecular dynamics runs.

$$V_{\text{wall}}(r) = \begin{cases} \infty & z \leq 0 \\ 0 & z > 0, \end{cases} \quad (16)$$

$$V_{\text{sphere}}(r) = \begin{cases} \infty & r \leq r_{\text{sphere}} \\ 0 & r > r_{\text{sphere}}. \end{cases} \quad (17)$$

The same closures were used in these calculations as were used above, although the discretization was not as fine ($\sim 0.10\sigma$). For purposes of comparison, these calculations were also done at conditions of $T^* = 1.0$ and $\rho^* = 0.73$.

In Fig. 11 we show the force curves between hard spheres of several different radii and the hard wall. The most striking thing about these curves in comparison with our previous results is that they are always (almost)

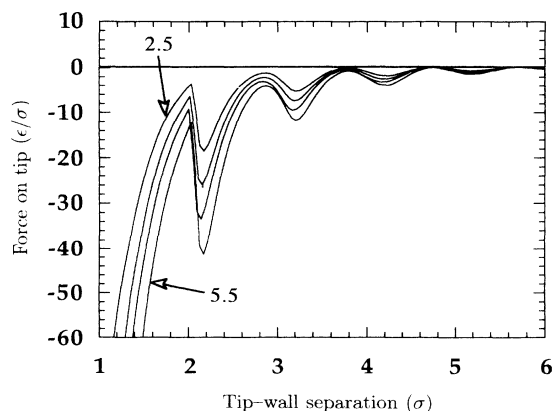


FIG. 11. Force-distance curves for the hard-wall-hard-sphere system, for several different sizes of sphere at a bulk liquid density of $\rho^* = 0.73$, and a reduced temperature $T^* = 1.0$. The sphere radii are 5.5σ , 4.5σ , 3.5σ , and 2.5σ . These results were obtained by solving the integral equations.

negative; the tip is pulled toward the wall by an oscillatory but increasing (in magnitude) force as it is brought nearer. This can be explained by considering the energetics of a Lennard-Jones fluid near a hard surface. A molecule very near the surface (within 1σ of contact) has fewer than its usual 12 nearest neighbors because the wall excludes them (for a close-packed solid near a wall, it would have exactly nine neighbors) and so pays an energetic penalty for being near the wall. We can expect to see "hydrophobic" behavior in the fluid because of this. In this system, when we create a highly constrained environment (under the tip) by moving the tip near the surface, a low-density liquid should evacuate this region, and the pressure of the liquid on the top of the sphere should push it toward the surface. In a dense liquid the volume under the tip will still be occupied, and the packing behavior mentioned earlier will still be observed, but the oscillations will be superimposed on a net attractive force curve. As one might expect from the smaller density oscillations near the hard wall, not as many force oscillations are observed in the hard-wall-hard-sphere system as in the Steele system.

This kind of behavior would be difficult to observe experimentally. If, in a physical system with similar potentials, one tried slowly to lower the tip toward the surface, it would be pulled toward contact as soon as it "sensed" the surface, (with increasing force) and only a single jump would be observed. The tip *should* jump from one force-distance peak to the next (and we would see a stepped curve), but if the noise in the system is of sufficient magnitude, these individual jumps would not be detected. Likewise, if one tried slowly to pull the tip away from contact with the surface, by applying enough force to remove it a small distance, one would (without extremely fine control) immediately pull it quite far away from the surface. Thus one could measure the *adhesion* force induced by the liquid between the two solids, but not the oscillatory force at longer ranges. This may explain the results of the atomic-force-microscope measurements on water mentioned above. Since graphite and silicon nitride (the tip material) are reasonably hydrophobic materials (at least, the water-water interactions are much stronger than the water-surface interactions) the water system is roughly similar to our hard-surface system, and so the oscillatory force curve may still be there, but invisible to the kind of measurements being made.

In these simulations the tip and surface are structureless. In order to model the atomic force microscope more realistically we should introduce structure into these and also include the London forces acting between the tip and surface. A more elaborate simulation of the atomic-force-microscope system might model the tip with a mobile (but heavy) sphere attached to a spring of some fairly large force constant acting in the z direction. Instead of moving the sphere itself, one would move the potential minimum of the spring up and down, allowing the sphere to find its own equilibrium separation. This system might reproduce the "jumps" seen in the experiments of Horn and Israelachvili on OMCTS, and in the measurements on water mentioned above. Our integral equation theory would not be applicable to such a system,

since (in our formulation) $V_{23}(r)$ would vary with sphere-wall separation, and so we would need to solve a system of three equations, rather than two. Molecular dynamics could certainly be used to study this system, but would certainly require much longer equilibration times than the simulations performed so far, and this work has not yet been attempted. It will be worthwhile to do such simulations, but we believe that the current model describes the essential physics of the solvation force effects.

Since hard walls are not physically realistic, except for very large-scale systems, we repeated these calculations for a “weak-walled” system where the wall potential and sphere potential have the same form as in the MD simulations and the first group of approximate theory calculations, but scaled down by a factor of 10. That is, the potential well depth near the wall or sphere is only about 0.3ϵ rather than 3.0ϵ , so that in this system the liquid-liquid interactions should dominate the liquid-wall interactions. All calculations were performed using the same state points as used in the hard-wall calculations. The results for spheres with several different radii are shown in Fig. 12. These curves are quite similar to those of the hard-wall system; the force curve is principally negative, and the same number of oscillations are visible. Comparing Fig. 12 with Fig. 11 (the hard-wall force curves) we see that the weak-wall curves are shifted up from the hard-wall ones, and that the oscillations are of similar magnitude. Essentially, the weak-wall force curves interpolate between those from the hard-wall system and those from our original system. Such comparisons allow us to resolve the force curve into a sum of two parts; an oscillatory force that arises entirely from the liquid structure, and a monotonically increasing force that arises from surface-liquid interactions. The stronger the surface-liquid interactions, the more the force curve is shifted up at small separations, since for a deeper potential well the system should favor a larger tip-wall separation because more liquid could occupy the well. A continuum-liquid model should show a smooth force

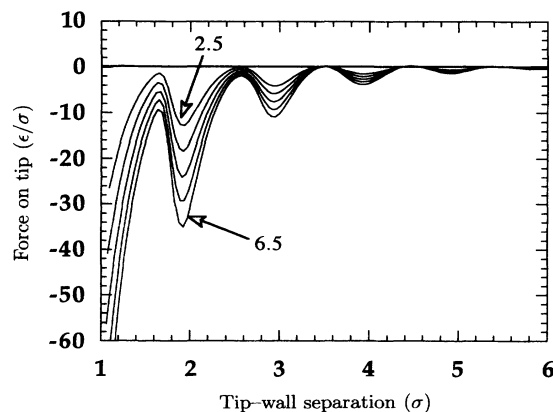


FIG. 12. Force-distance curves for the “weak-wall” system, for several different sizes of sphere at a bulk liquid density of $\rho^*=0.73$, and a reduced temperature of $T^*=1.0$. The sphere radii are 6.5σ , 5.5σ , 4.5σ , 3.5σ , and 2.5σ . These results were obtained by solving the integral equations.

curve that increases with decreasing separation (up to some contact value), with magnitude dependent on the surface-liquid interaction strength.

IV. CONCLUSIONS

By performing molecular dynamics simulations on a very simple model of an atomic-force-microscope tip in a liquid, we obtain force vs distance curves that are in good qualitative agreement with experiment. Also, we may generate such curves by the much less computationally expensive route of applying the integral equation theory to our model, and obtain reasonable agreement between these two methods. We have previously explained these oscillatory force curves in terms of the density profiles of the solvent in the region under the tip, and have demonstrated that the observed liquid structures at various tip-wall separations correlate well with the features in the force curve.

We may compare these results, both from molecular dynamics simulations and the integral equation theory, with experimental results. Looking at the atomic-force-microscope data of O’Shea, Welland, and Rayment, we see five or six oscillations superimposed on a net attractive force. We cannot really make judgments as to the decay rate of these oscillations, since the spread in the data is quite large, but the amplitude of the oscillations is on the order of 0.3 nN. If we attempt to scale our reduced Lennard-Jones parameters to the OMCTS system, from using the heat of vaporization of OMCTS $\Delta H_{\text{vap}}=48.179$ kJ/mol (Ref. 16) and taking $\Delta H_{\text{vap}}/\text{atom}=8.16\epsilon$ (the lattice energy for the perfect fcc Lennard-Jones crystal)¹⁷ we get $\epsilon=673.3$ K= 9.29×10^{-21} J and $\sigma \approx 8$ Å. From the molecular dynamics simulation of the 5σ sphere system, the amplitude of the first oscillation (the difference between the second maxima and the first minima) is approximately $31.5 \sigma/\epsilon$, which becomes 3.65×10^{-10} N or 0.365 nN. This is of the same order of magnitude as the experimental result. Considering the approximations made in the choice of the liquid-surface and liquid-liquid potentials, and the unknown size of the experimental tip, any quantitative agreement is probably coincidental.

Principally by using results of the integral equation theory, but also corroborated by molecular dynamics simulations, we have observed the effect that tip size has on these force-distance curves. The amplitude of the force oscillations is found to vary linearly with the sphere radius, and the number of oscillations present in the force curve is *not* particularly sensitive to tip size. This is because a larger tip would not be expected to have a much longer-ranged effect on solvent structure than a smaller one. This linearity is not entirely surprising; Horn and Israelachvili have observed it in experiments with the surface force apparatus. We have found that, although the force-distance curves resulting from this integral equation theory and molecular dynamics simulations are very similar, the slopes they yield for the linear relationship between the force on the sphere and radius of the sphere are quite different (particularly for the first oscillation), due to the failure of the theory at very small separations.

This relationship could be used to determine the relative sizes of atomic-force-microscope tips. By using different tips to measure the force-distance curve of a solvent such as OMCTS, one could obtain the contact area of one tip relative to another, by comparing the amplitudes of the second or third force oscillations. Since the first oscillation has been shown to deviate from this linearity, only later oscillations should be used for this purpose. Furthermore, by comparing with the data obtained by Horn and Israelachvili [who measured $F(R)$ vs R], one could estimate the absolute radius of the tip. Real tips are irregular, but these results show that the force curves are determined only by the part of the tip which is nearest the flat surface.

We have also used the integral equation theory to look at the force-distance behavior for different state points of the liquid. We find that increasing temperature causes a decrease in the magnitude of the oscillations. Increasing the liquid density is found to increase the magnitude of the oscillations, as well as slightly to decrease their wavelength.

Applying the integral equation theory to systems with different surface-liquid potentials has allowed us to see the way that liquid-surface interactions and liquid-liquid interactions are separately related to the total force felt by the tip. The oscillations arise from the liquid structure, and are not strongly affected by varying the liquid-surface potential well depth, while the curve upon which these oscillations are imposed is very dependent on the liquid-surface potential. It may also be very dependent on the liquid-liquid potential, but we have not yet studied systems with liquid-liquid potentials other than the Lennard-Jones, and the scaling properties of that potential make considerations of absolute well depth inconsequential.

ACKNOWLEDGMENTS

We thank Dr. T. Rayment for useful discussions, SERC for support (Grants Nos. GR/H 68529 and GR/H 04190), and the Marshall Aid Commemoration Commission for their support of L.D.G. in this work.

¹S. J. O'Shea, M. E. Welland, and T. Rayment, *Appl. Phys. Lett.* **60**, 2356 (1992).

²R. G. Horn and J. N. Israelachvili, *J. Chem. Phys.* **75**, 1400 (1981).

³J. J. Magda, M. Tirrell, and H. T. Davis, *J. Chem. Phys.* **83**, 1888 (1985).

⁴I. K. Snook and W. van Megen, *J. Chem. Phys.* **72**, 2907 (1980).

⁵L. J. Douglas, M. Lupkowski, T. L. Dodd, and F. van Swol, *Langmuir* **9**, 1442 (1993).

⁶R. Kjellander and S. Sarman, *Mol. Phys.* **70**, 215 (1990).

⁷F. A. Abraham, *J. Chem. Phys.* **68**, 3713 (1978).

⁸L. D. Gelb and R. M. Lynden-Bell, *Chem. Phys. Lett.* **211**, 328 (1993).

⁹D. Henderson and M. Plischke, *J. Chem. Phys.* **97**, 7822 (1992).

¹⁰W. A. Steele, *Surf. Sci.* **36**, 317 (1973).

¹¹H. J. C. Berendsen, J. P. M. Postma, W. F. DiNiola, A. van Gunsteren, and J. R. Haak, *J. Chem. Phys.* **81**, 3684 (1984).

¹²M. P. Allen and D. J. Tildesley, *Computer Simulation of Liquids* (Clarendon, Oxford, 1987).

¹³J. P. Hanse and I. R. McDonald, *Theory of Simple Liquids* (Academic, New York, 1976).

¹⁴G. Zerah, *J. Comp. Phys.* **61**, 280 (1985).

¹⁵D. Henderson, F. F. Abraham, and J. A. Barker, *Mol. Phys.* **31**, 1291 (1976).

¹⁶R. C. Weast, and M. J. Astle, *Handbook of Chemistry and Physics*, 62nd ed. (Chemical Rubber Company, Boca Raton, FL, 1981).

¹⁷E. R. Dobbs and G. O. Jones, *Rep. Prog. Phys.* **20**, 516 (1957).

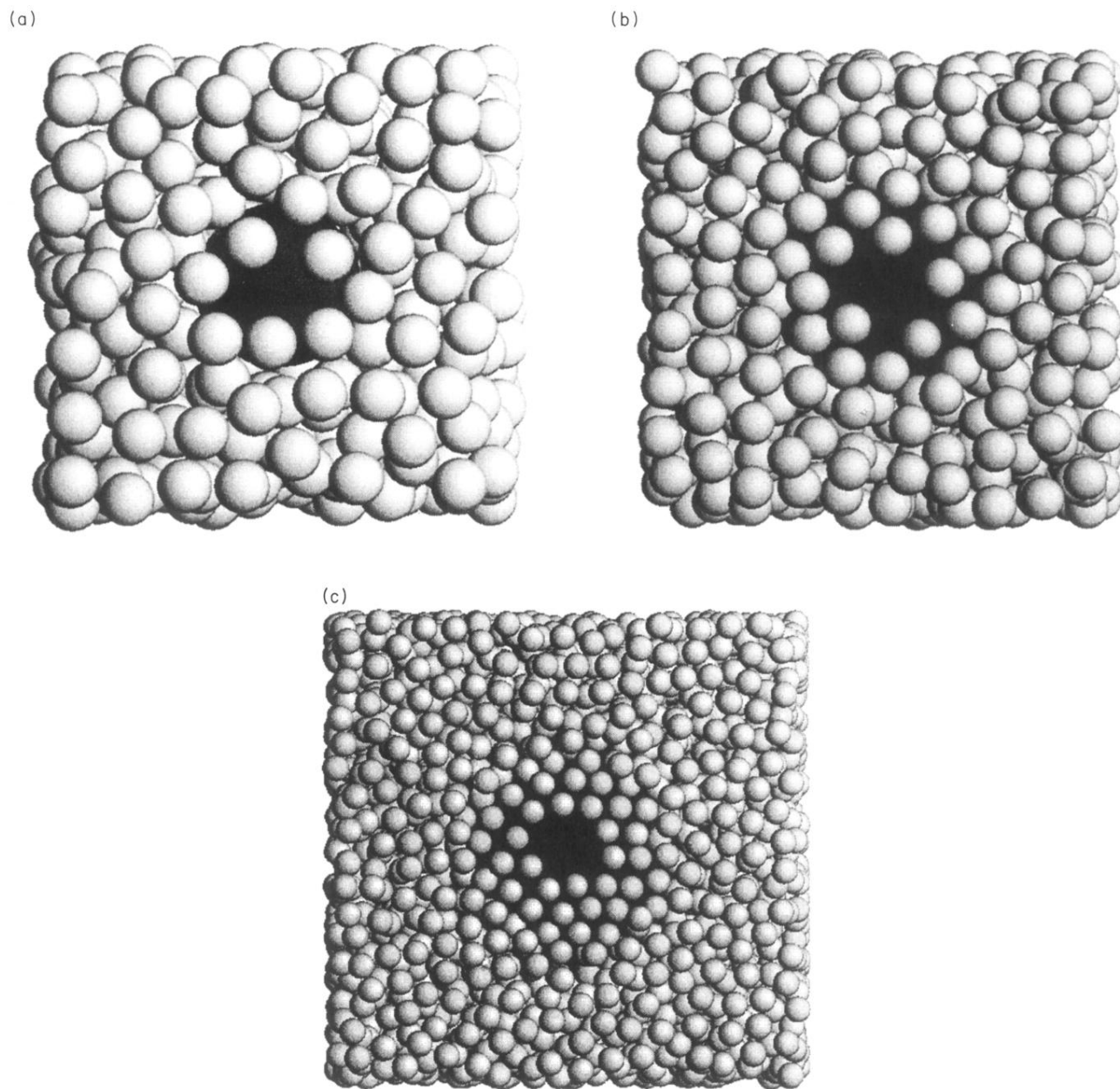


FIG. 4. Representative molecular-dynamics configurations from all three diameter sphere simulations, each at a tip-wall separation of 1.75σ . (a) is from the 3σ diameter sphere run, (b) is from 5σ sphere run, and (c) is from the 11σ sphere run. In each case, the viewpoint is from the center of the bottom surface, looking up along the z axis. In other words, the topmost layer of visible atoms in each configuration is the first solvation layer alongside the flat surface.